Singular Field Response and Singular Screening of Vacancies in Antiferromagnets

Alexander Wollny, Eric C. Andrade, and Matthias Vojta
Institut für Theoretische Physik, Technische Universität Dresden, 01062 Dresden, Germany
(Received 22 June 2012; published 23 October 2012)

For isolated vacancies in ordered local-moment antiferromagnets we show that the magnetic-field linear-response limit is generically singular: The magnetic moment associated with a vacancy in zero field is different from that in a finite field h in the limit $h \to 0^+$. The origin is a universal and singular screening cloud, which moreover leads to perfect screening as $h \to 0^+$ for magnets which display spin-flop bulk states in the weak-field limit.

DOI: 10.1103/PhysRevLett.109.177203 PACS numbers: 75.10.Jm, 75.10.Nr, 75.50.Ee

Defects are ubiquitous in solids. In magnets with localized spin moments, typical classes of defects are missing or extra spins, arising, e.g., from substitutional disorder. Very often, even small concentrations of such defects produce a large magnetic response at low temperatures: Quasifree spins cause a Curie tail in the magnetic susceptibility, which then is routinely subtracted from raw experimental data. Assuming independent defects, the amplitude of the Curie tail can be utilized to estimate the defect concentration, provided that the behavior of a single defect is known.

Here we discuss the physics of isolated vacancies in antiferromagnets (AFs) which display semiclassical long-range order (LRO) in the ground state [1]. In zero magnetic field, the state with a single vacancy has a finite uniform magnetic moment, m_0, because the vacancy breaks the balance between the sublattices. For collinear magnets, m_0 is quantized to the bulk spin value, $m_0 = S$ [2,3], while in the noncollinear case fractional values of m_0 occur due to the local relief of frustration [4]. These vacancy moments are expected to show up in magnetization measurements, and they produce a low-temperature Curie contribution to the uniform susceptibility in the two-dimensional (2D) case where bulk order is prohibited by the Mermin-Wagner theorem [3–7].

In this Letter we show that, in an applied field h, nontrivial screening of the vacancy moment occurs, such that the linear-response limit $h \to 0^+$ is *singular* for a magnet with a single vacancy, Fig. 1: The vacancy-induced magnetization jumps discontinuously from its zero-field value m_0 to a different value $m(h \to 0^+)$ upon applying an infinitesimal field h. Thus, measurements of the vacancy-induced moment $m(h)$ in a finite field h cannot detect the zero-field value m_0 even for small h [8], which is of obvious relevance for any experiment trying to quantify the defect contribution to a sample's magnetization or susceptibility. Furthermore, the spin texture around the vacancy at finite h has a piece [9] which is singular as $h \to 0^+$—in a sense made precise below—which screens the vacancy-induced moment perpendicular to $\vec{h}$. For magnets which feature spin-flop states (with all spins perpendicular to $\vec{h}$ as $h \to 0^+$) in the absence of the vacancy, this leads to a semiclassical version of *perfect screening* of the vacancy moment, $m(h \to 0^+) = 0$.

In the body of this Letter, we present general arguments and microscopic calculations supporting these claims. Explicit results will be given in a $1/S$ expansion for spin-S AFs on 2D lattices, with

$$\mathcal{H} = J \sum_{\langle ij \rangle} \vec{S}_i \cdot \vec{S}_j - h \sum_i S_i^z, \tag{1}$$

but our results are valid for AFs with LRO in any dimension d. In particular, the singular response occurs for vacancies in the square-lattice AF, where—despite numerous studies [6,7,9–13]— it has been overlooked to date [14]. The singular behavior will be cut off for a finite vacancy density, and we shall discuss the resulting crossover scales [8].

Bulk behavior in a field.—To set the stage, we recapitulate the evolution of a bulk AF state, which spontaneously breaks the underlying SU(2) symmetry, upon application of a uniform field. As $h \neq 0$ breaks the symmetry down to U(1), an infinitesimal field typically selects a subset of states, which we refer to as $h \to 0^+$ bulk states: For the

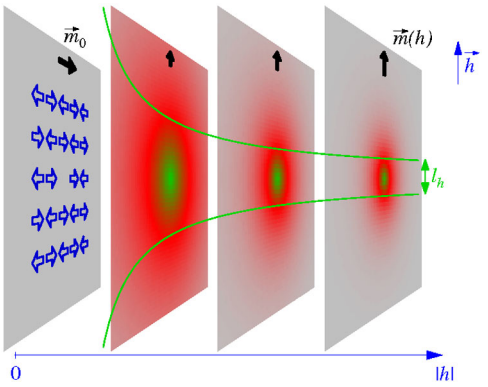

FIG. 1 (color online). Illustration of singular screening for the square-lattice AF: At zero field, the vacancy induces a moment $\vec{m}_0$ with $m_0 = S$, which is modified into $\vec{m}(h)$ in the presence of a uniform field $\vec{h}$. The size of the screening cloud, l_h, diverges as $h \to 0^+$, and $m \to 0$ in this limit. For details see text.

square lattice, these are spin-flop states with staggered spin directions perpendicular to $\vec{h}$. With increasing field the spins rotate toward the field direction, until a fully polarized state is reached, see the illustration in Fig. 2(a).

For the triangular-lattice AF, an anomalously large ground-state degeneracy exists at the classical level for $h \neq 0$, which is lifted both by fluctuations and by additional interactions [15–18]. Two cases are important: (a) *coplanar* and (b) *umbrella* states, see Fig. 3. In (a) the spins are oriented in a plane in the field direction, and the evolution is via an intermediate up-up-down magnetization plateau (with a bulk magnetization of $1/3$ of the saturation value). In contrast, in (b) the spins are arranged in planar spin-flop states perpendicular to the field for $h \to 0^+$, and evolve in a noncoplanar fashion continuously towards full polarization. Below, we shall employ an additional biquadratic exchange $K\sum_{\langle ij\rangle}(\vec{S}_i \cdot \vec{S}_j)^2$ with relative strength $k = KS^2/J$ to select between the two cases in a classical calculation: $k > 0$ ($k < 0$) favors umbrella (coplanar) states, with $|k| < 2/9$ required to preserve the familiar 120° order at zero field [18].

Numerical results.—We now present numerical results for the single-vacancy finite-field ground state of square and triangular AFs. We consider the vacancy contribution to the magnetization, $m(h)$, defined as the difference between the total magnetizations of the system with and without vacancy. Figures 2 and 3 display $m(h)$ for the classical AF on the square and triangular lattices and demonstrate our main results: (i) $m(h \to 0^+)$ does not reach the zero-field moment $|m_0|$ in any of the cases, i.e., the impurity magnetization jumps upon application of an infinitesimal field; (ii) for the square lattice we find $m(h \to 0^+) \to 0$; the same happens for umbrella states in the triangular lattice. In contrast, $m(h \to 0^+)$ tends to a finite value in the coplanar triangular-AF case. Figure 2(a) also shows the next-to-leading term in a $1/S$ expansion for $m(h)$, indicating that quantum corrections do not qualitatively change these results.

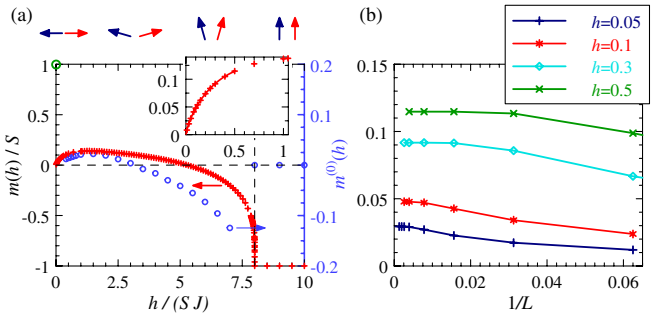

FIG. 2 (color online). Vacancy contribution to the uniform magnetization, $m(h)$, for the square-lattice AF. (a) Crosses: classical result $m(h)/S$, obtained on lattices with $L \leq 768$ and extrapolated to $L \to \infty$; the circle shows the linear-response value $|m_0/S| = 1$. Open dots: $1/S$ correction $m^{(0)}(h)$, here $L \leq 50$. Vertical dashed line: saturation field $h_{\rm sat} = 8SJ$ [23]. Top arrows: evolution of the bulk spin state with increasing h. Inset: small-h behavior of $m(h)/S$, together with a fit $m \propto h \ln h$ (see text). (b) Finite-size data $m(h)/S$ as function of $1/L$. m saturates for $L > l_h$ with $l_h \propto SJ/h$.

In the remainder of the Letter we explain the physics behind these striking observations. As a first step, we show that the spin configurations are necessarily different for $h = 0$ and $h \to 0^+$ in the presence of a vacancy.

Vacancy: Zero-field state.—The vacancy breaks the balance between the sublattices of the host AF and locally distorts the bulk state. If the AF is collinear (and remains collinear upon introducing the vacancy) there is no distortion in the classical limit, and the vacancy-induced magnetization is $m_0 = S$. Quantum fluctuations arise from the action of $S_i^+ S_j^-$ terms in the Hamiltonian and hence conserve total spin, such that m_0 remains locked to S; however, the amplitudes of the $\langle \vec{S}_i \rangle$ are modified near the vacancy. In noncollinear AFs, the directions of the $\langle \vec{S}_i \rangle$ readjust in response to the vacancy because frustration is locally relieved. Then, m_0 takes a fractional value which depends on S and microscopic details [4]; i.e., the vacancy spin gets partially screened, and both undercompensation and overcompensation are possible.

In all cases, the local distortions decay algebraically with the distance r to the vacancy due to the presence of Goldstone modes. Typically this decay follows $1/r^{d+1}$ [4,11], such that the total (i.e., integrated) vacancy contribution to any observable is bounded, i.e., of order unity—this we refer to as a *regular* screening cloud.

Singular $h \to 0^+$ limit.—Now consider applying an infinitesimal field $\vec{h}$. To this end, rotate the $h = 0$ state in spin space such that the spins far away from the vacancy match a $h \to 0^+$ bulk configuration. This generates a state with finite magnetization $\vec{m}_0$ which, however, is in general *not* oriented in the field direction. This is illustrated in Fig. 1 for the square lattice, where the spins are oriented

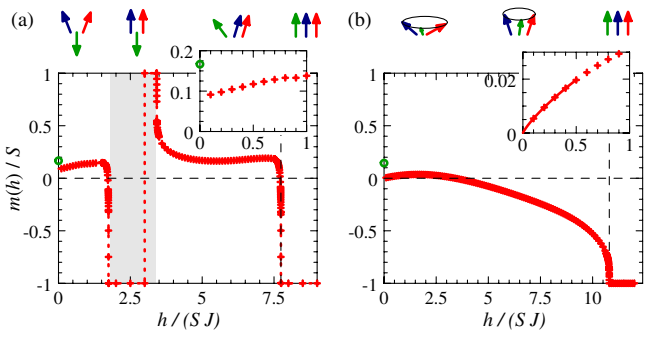

FIG. 3 (color online). Vacancy-induced magnetization as in Fig. 2, but for the classical triangular-lattice AF with biquadratic exchange of strength (a) $k = -0.07$, leading to coplanar states in a field, and (b) $k = 0.1$, leading to umbrella states. Here $h_{\rm sat} = 9SJ(1 + 2k)$, the shaded area in (a) indicates the magnetization plateau. Insets: small-h behavior. Note that m_0 takes a k-dependent fractional value [4].

perpendicular to the infinitesimal field—the same applies to $\vec{m}_0$. Clearly, such a state *cannot* be the ground state for $h \neq 0$, as stability demands $\vec{m} \parallel \vec{h}$ in the presence of SU(2) symmetry. In other words, the states at $h = 0$ and $h \to 0^+$ are required to differ because the latter is subject to the additional constraint that the uniform moment has to point in field direction (while both states have matching spin directions far away from the vacancy). Fulfilling this constraint requires an additional distortion to screen the moment perpendicular to $\vec{h}$.

This analysis also reveals exceptions *without* zero-field singularity in the presence of a vacancy: This happens when the properly rotated zero-field state has a moment $\vec{m}_0$ which points along the direction of the infinitesimal $\vec{h}$. A concrete example is the triangular lattice with coplanar states and undercompensated impurity moments [4]. (In the classical limit, there is overcompensation for all $k < 0$ [4] which leads to results as in Fig. 3(a), but undercompensation can be expected for $S < \infty$.)

We note that mean-field theory, neglecting spatial variations and thus distributing the screening process over the entire system, qualitatively reproduces the zero-field singularity in $m(h)$, but fails in other respects [19].

Finite-field screening cloud.—We turn to the finite-field screening, in order to understand the difference between the cases in Figs. 2(a) and 3(a), where $m(h \to 0^+)$ reaches zero or a finite value, respectively. The vacancy-induced modification of the directions of $\langle \vec{S}_i \rangle$ can be parameterized by the spherical angles $\delta\Theta_i$, $\delta\phi_i$ [one angle is sufficient for the coplanar cases in Figs. 2(a) and 3(a)]. Considering that the distortion serves to screen the vacancy moment's component perpendicular to $\vec{h}$, the screening can be quantified using

$$\vec{m}_\perp(r) = \sum_{|\vec{r}_i| \leq r} \langle \vec{S}_i \rangle_\perp, \tag{2}$$

where $\langle \vec{S}_i \rangle_\perp$ is the moment perpendicular to $\vec{h}$, and the sum runs over all sites with a distance to the vacancy closer or equal r. Clearly, $\vec{m}_\perp(r \to \infty)$ is the total magnetization perpendicular to $\vec{h}$ and has to vanish.

We start with the square lattice: The angles $\delta\Theta$, Fig. 4(a), decay exponentially on a length scale $l_h \propto SJ/h$. This is expected: The distortion is mediated by a bulk mode which is a gapless Goldstone mode in zero field, but acquires a gap $\propto h$ for $h > 0$. A remarkable feature is that $\delta\Theta_i$ at fixed $\vec{r}_i$ has a nonmonotonic field dependence and appears to reach zero as $h \to 0$ (visible at small r). This implies that the distortion, and with it the screening, happens at progressively larger r with decreasing h. This is confirmed by the plot of $\vec{m}_\perp(r)$, Fig. 4(c), showing that the cloud size increases as $h \to 0^+$.

To understand these results analytically, we resort to a continuum description: The small-field distortions consist of smooth variations of the order-parameter field $\vec{\varphi}(\vec{r})$

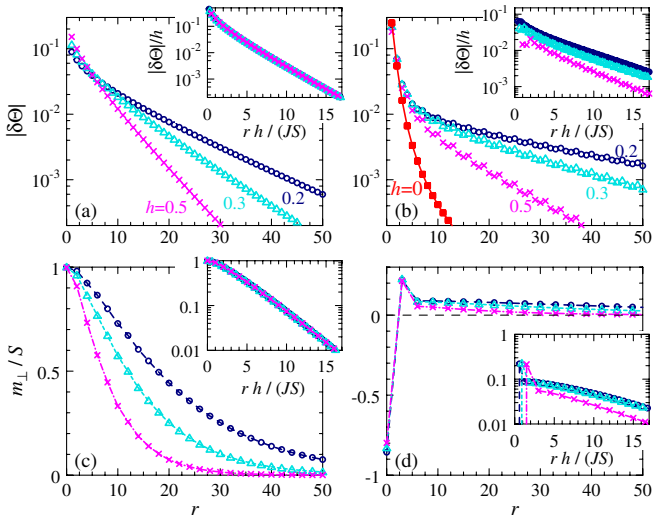

FIG. 4 (color online). Field-induced screening cloud for [(a), (c)] the square lattice and [(b), (d)] the triangular lattice with $k = -0.07$, for different values of h. (a), (b) Vacancy-induced rotation angles $\delta\Theta(\vec{r})$ as a function of the distance r to the vacancy. In (b) the zero-field angles are shown as well. Insets: scaling of $\delta\Theta/h$ vs $rh/(SJ) \propto r/l_h$, with the short-range piece projected out in (b). (c), (d) Transverse magnetization $\vec{m}_\perp(r)$ as a function of the integration radius r in Eq. (2). Insets: $\vec{m}_\perp$ vs rescaled distance $rh/(SJ)$.

(or, equivalently, of the angles Θ on all sublattices). For a single vacancy, those distortions have been analyzed in Ref. [9], and found to decay as $h^{d-1}/(\rho_s c^{d-2}) f_d(hr/c)$ where ρ_s and $c \propto SJ$ are the spin stiffness and spin-wave velocity, respectively, and f_d is a universal function which depends on the dimension d only. Specifically, $f_2(x) = K_0(x)$ (the modified Bessel function), and $f_3(x) = \exp(-x)/x$.

To analyze the screening of $m_\perp$, we first note that distortion-induced (local) contributions to $m_\perp$ arise—in the presence of a finite bulk magnetization density $\vec{l} \propto \vec{h}$ – to linear order in $\delta\Theta$, $\delta m_\perp \propto \int d^d r |\vec{l}| \delta\Theta$, which have to compensate the bare vacancy-induced transverse moment (which itself equals S in the square-lattice case). Using the above long-distance form of the distortion, we have $\delta m_\perp \propto (c^2/\rho_s)(h/c)^d \int d^d r f_d(hr/c) \propto (c^2/\rho_s) \int d^d x f_d(x)$. As the last integral is finite, we see that all h dependence has dropped out, indicating stable screening of $m_\perp$ for any h.

The insets in Figs. 4(a) and 4(c) confirm the anticipated scaling of our data with l_h: Plotting $\delta\Theta/h$ and $\vec{m}_\perp$ each as a function of rescaled distance $rh/(SJ)$ reveals data collapse; i.e., the screening cloud is *universal* for small fields. The scaling of $\delta\Theta/h$ also implies that the texture does not approach a well-defined limiting form as $h \to 0^+$, but instead has a diverging size combined with a vanishing amplitude—this we refer to as a *singular* screening cloud.

A similar calculation can be employed to obtain the cloud's contribution to the field-parallel magnetization

$m_\parallel \equiv m(h)$. This arises from two higher-order terms, $\int d^d r |\vec{l}| \delta\Theta^2$ and $\int d^d r |\vec{\varphi}| \vec{\nabla}^2 \Theta$, while lower orders vanish because the transverse magnetization density is zero in the bulk reference state. The first term scales as $h^{d-1} \int d^d x f_d^2(x)$ while the second one scales as $h \int d^d x f_d''(x)$. Importantly, the first integral is regular whereas the second one has a short-distance logarithmic divergence in any d—this is cut off by noting that the lower limit of the x integral is not zero, but $\propto h$. As a result, the cloud's contribution to $m(h)$ follows $(h \ln h)$ for small h. Indeed, our numerical results in Fig. 2(a) are perfectly fit by this form—note that the bare vacancy-induced moment along $\vec{h}$ vanishes $\propto h$ and is subleading.

Now we turn to the triangular lattice. An analysis of the angles $\delta\Theta(r)$, Fig. 4(b), shows that they arise from a superposition of two textures, with spatial s-wave and f-wave symmetries, respectively. The latter is well localized near the vacancy and evolves smoothly into the zero-field texture [4], while the former is a field-induced distortion very similar to that in the square lattice. As a result, we find two-stage screening at small h: At short distances, the moment of the missing spin is screened to $\vec{m}_0$ in a regular and weakly field-dependent fashion, while the field-perpendicular component of this $\vec{m}_0$ is then compensated at larger distances via a singular cloud of size l_h. This singular piece can be isolated by projecting $\delta\Theta(r)$ onto its s-wave component, Fig. 4(b), and it admits the same continuum description as above. Because of the nearby magnetization plateau, universal scaling is reached at much smaller h as compared to the square lattice.

Finally, this insight allows us to deduce the value $m(h \to 0^+)$: This is simply the field-parallel part of $\vec{m}_0$ in the (properly rotated) zero-field state, because the contribution of the singular screening cloud vanishes as $(h \ln h)$. For the triangular lattice with overcompensated impurity, this $\vec{m}_0$ forms a 60° angle with $\vec{h}$ [4] such that $m(h \to 0^+) = |\vec{m}_0|/2$, matching our numerical result in Fig. 3(a), while for all systems with spin-flop states $m(h \to 0^+) = 0$; i.e., the vacancy moment is perfectly screened.

Quantum effects.—Although the concrete calculations so far were for classical spins, the results qualitatively apply to any system with semiclassical LRO: As happens in general for noncollinear magnets, quantum effects will modify directions and amplitudes of $\langle \vec{S}_i \rangle$. However, the existence of both the zero-field singularity and the perfect screening are unaffected, as they derive from symmetry and stability arguments.

To illustrate this, we have calculated quantum corrections to $m(h)$ in a $1/S$ expansion using spin-wave theory on finite lattices [20–22]. A sample result for the next-to-leading term ($\propto S^0$) of $m(h)$ for the square lattice is shown in Fig. 2 [23]—its $h \to 0$ behavior is consistent with $(h \ln h)$.

Limits and crossover scales.—The zero-field singularity only occurs in the thermodynamic limit [8]: m evolves smoothly for a single vacancy in a finite-size system with $N = L^d$ sites, and the limits $N \to \infty$ and $h \to 0$ do not commute [19].

Assuming now a finite vacancy concentration n_{imp}, the singularity is replaced by a crossover governed by the two length scales l_h and $l_{\text{imp}} = n_{\text{imp}}^{-1/d}$, the mean vacancy distance. For $l_h \ll l_{\text{imp}}$, the vacancy moments respond independently to the field, whereas for $l_h \gg l_{\text{imp}}$ the screening clouds overlap and hence their moments tend to average out (for an equal distribution over all sublattices). Thus, the magnetization per vacancy will follow $m(h)$ as calculated here for elevated fields, but will (smoothly) vanish below a crossover field given by $h/J \sim n_{\text{imp}}^{1/d}$.

These considerations also apply at finite temperatures inside the ordered phase of 3D Heisenberg magnets. In 2D, order occurs only at $T = 0$, but the bulk correlation length ξ becomes exponentially large as $T \to 0$. Then, the physics is governed by the interplay of the three length scales l_h, l_{imp}, and ξ, and we quickly discuss some interesting limits. For $\xi \gg l_h, l_{\text{imp}}$ one recovers the $T = 0$ physics discussed above. Single-impurity physics obtains in the dilute limit, $l_{\text{imp}} \gg \xi, l_h$, where at elevated fields, $\xi \gg l_h$, the magnetization per vacancy again follows our $m(h)$. In contrast, in the low-field limit, $\xi \ll l_h$, linear response is restored such that the vacancy susceptibility takes the Curie form $\chi = m_0^2/(3kT)$ [3–7]; i.e., the singularity is replaced by a crossover on the scale $h/J \sim \exp(-T/J)$. Finally, the limit $l_h \gg \xi, l_{\text{imp}}$ is governed by zero-field physics.

Conclusions.—For a single vacancy in an ordered AF we have found that the magnetic behavior is generically singular in the weak-field limit: The vacancy contribution to the magnetization jumps discontinuously upon applying an infinitesimal field. The singularity can be traced back to nontrivial field-induced screening due to a universal and singular screening cloud in the $h \to 0^+$ limit.

Our predictions can be experimentally verified in any AF doped with a small, controlled amount of vacancies, provided that magnetic anisotropies are small [8]. In addition, numerical studies beyond the $1/S$ expansion (e.g., quantum Monte Carlo calculations) are called for.

We thank J. Kunes, R. Moessner, and O. I. Motrunich for discussions, and L. Fritz for collaboration at an early stage of this work. This research was supported by the DFG through FOR 960 and GRK 1621.

[1] S. Chakravarty, B. I. Halperin, and D. R. Nelson, Phys. Rev. B **39**, 2344 (1989).
[2] A. W. Sandvik, E. Dagotto, and D. J. Scalapino, Phys. Rev. B **56**, 11701 (1997).
[3] S. Sachdev, C. Buragohain, and M. Vojta, Science **286**, 2479 (1999).
[4] A. Wollny, L. Fritz, and M. Vojta, Phys. Rev. Lett. **107**, 137204 (2011).

[5] S. Sachdev and M. Vojta, Phys. Rev. B **68**, 064419 (2003).
[6] K. H. Höglund and A. W. Sandvik, Phys. Rev. Lett. **91**, 077204 (2003).
[7] O. P. Sushkov, Phys. Rev. B **68**, 094426 (2003).
[8] Violations of SU(2) symmetry remove the zero-field singularity, but only finite-h measurements along an easy axis can possibly detect the zero-field vacancy moment m_0.
[9] S. Eggert, O. F. Syljuasen, F. Anfuso, and M. Andres, Phys. Rev. Lett. **99**, 097204 (2007).
[10] N. Nagaosa, Y. Hatsugai, and M. Imada, J. Phys. Soc. Jpn. **58**, 978 (1989).
[11] A. Lüscher and O. P. Sushkov, Phys. Rev. B **71**, 064414 (2005).
[12] F. Anfuso and S. Eggert, Phys. Rev. Lett. **96**, 017204 (2006).
[13] S. Shinkevich, O. F. Syljuasen, and S. Eggert, Phys. Rev. B **83**, 054423 (2011).
[14] The $h \to 0$ singularity was observed numerically in Ref. [4] for a specific triangular-lattice case, but the generality and the underlying physics were not understood there.
[15] H. Kawamura and Y. Miyashita, J. Phys. Soc. Jpn. **54**, 4530 (1985).
[16] A. V. Chubukov and D. I. Golosov, J. Phys. Condens. Matter **3**, 69 (1991).
[17] L. Seabra, T. Momoi, P. Sindzingre, and N. Shannon, Phys. Rev. B **84**, 214418 (2011).
[18] A. Läuchli, F. Mila, and K. Penc, Phys. Rev. Lett. **97**, 087205 (2006).
[19] See Supplemental Material at http://link.aps.org/supplemental/10.1103/PhysRevLett.109.177203 for finite-system results and a discussion of a mean-field approach to vacancy-doped magnets.
[20] M. E. Zhitomirsky and T. Nikuni, Phys. Rev. B **57**, 5013 (1998).
[21] We employ the algorithm described in the appendix of S. Wessel and I. Milat, Phys. Rev. B **71**, 104427 (2005).
[22] For the triangular lattice at $k = 0$ we find $m_0 = -0.04S + 0.35 + \mathcal{O}(1/S)$, which corrects our earlier result in Ref. [4], where we missed the $1/S$ correction to the angles Θ_i [20].
[23] As $h \to h_{\rm sat}^-$, the classical-limit $m(h)$ is continuous with an infinite slope at $h_{\rm sat}$, associated with a diverging correlation length. Fluctuation corrections, already logarithmically singular without vacancy [20], require a more detailed analysis which is beyond the scope of this work.